

## ***Manganese as a Substitute for Rhenium in CO<sub>2</sub> Reduction Catalysts: The Importance of Acids.***

Jonathan M. Smieja, Matthew D. Sampson, Kyle A. Grice, Eric E. Benson, Jesse D. Froehlich, and Clifford P. Kubiak\*

Department of Chemistry and Biochemistry, University of California, San Diego, 9500 Gilman Drive, Mail Code 0358, La Jolla, California 92093–0358, United States

### **Table of Contents**

Figure S1	S2
Figure S2	S3
Figure S3	S3
Figure S4	S4
Figure S5	S4
Figure S6	S5
Table S1	S6
Costentin and Savéant TOF calculations	S7
Figure S7	S8
Table S3	S9
Table S4	S10

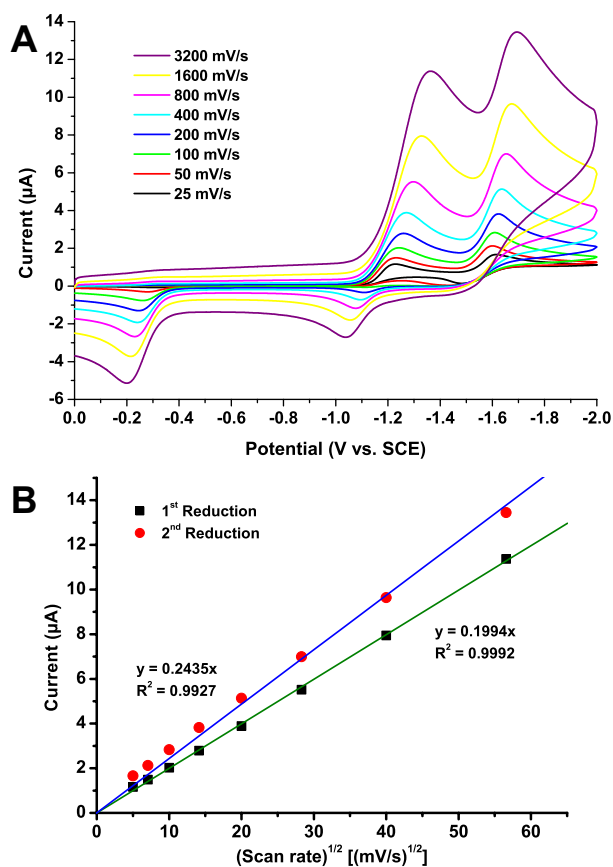


**Figure S1.** A.) Cyclic voltammogram scan rate dependence of 1 mM  $[\text{Mn}(\text{bpy-}t\text{Bu})(\text{CO})_3(\text{MeCN})](\text{OTf})$  (**3**) under an atmosphere of argon in acetonitrile. Electrochemical conditions were 0.1 M TBAH as supporting electrolyte, 1 mm diameter glassy carbon working electrode, Pt wire counter electrode, and Ag wire pseudo-reference electrode separated from the bulk solution by a Vycor tip. B.) Plot showing that current increases with the square root of the scan rate. This behavior is indicative of a freely-diffusing species where the electrode reaction is controlled by mass transport.

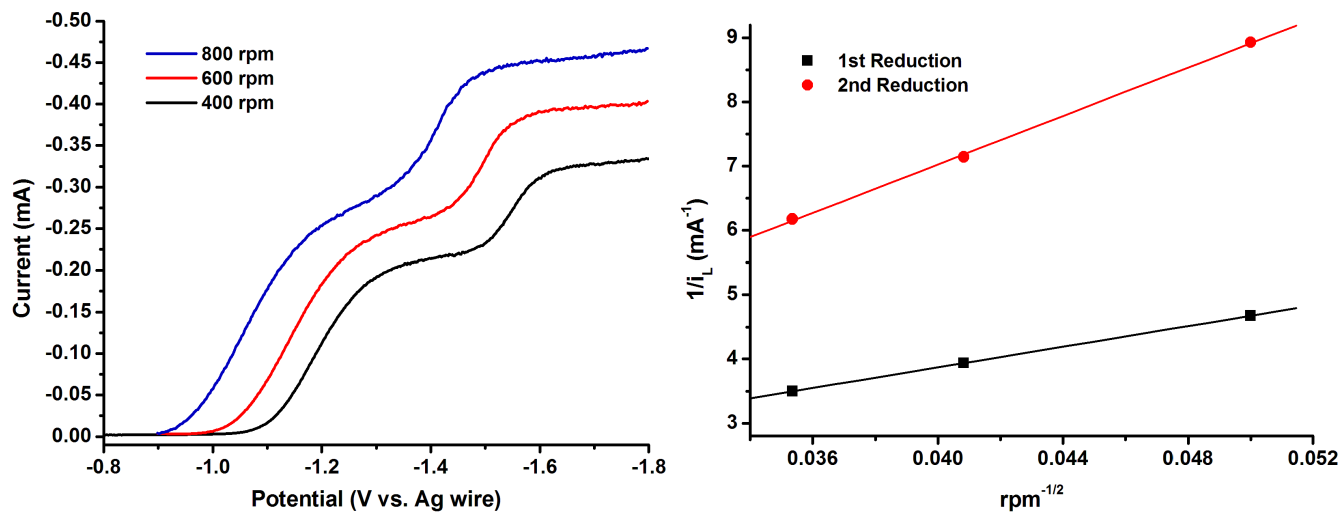


**Figure S2.** Rotating disk electrode data (left) and Levich-Koutecky plot (right) for 1 mM  $[\text{Mn}(\text{bpy-}t\text{Bu})(\text{CO})_3(\text{MeCN})](\text{OTf})$  (3) in MeCN with 0.1M TBAH as the supporting electrolyte under an atmosphere of argon.

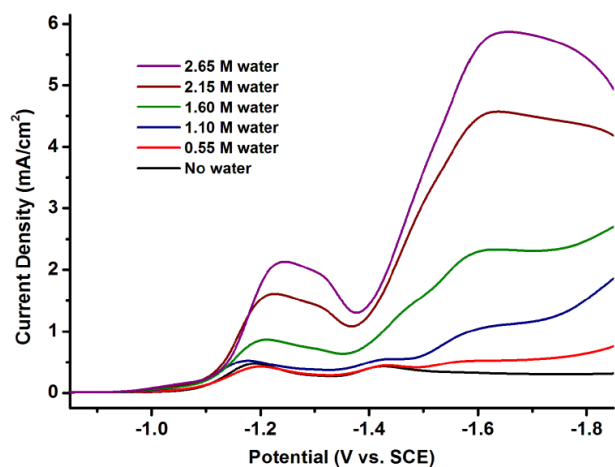


**Figure S3.** Linear scan voltammograms showing the electrocatalytic reduction of CO<sub>2</sub> to CO by 1 mM  $\text{Mn}(\text{bpy-}t\text{Bu})(\text{CO})_3\text{Br}$  (1) in acetonitrile with addition of water. Solution is under an atmosphere of, and saturated with (*ca.* 0.28 M), carbon dioxide. Electrochemical conditions were 0.1 M TBAH supporting electrolyte, 1 mm diameter glassy carbon working electrode, Pt wire counter electrode, and Ag wire pseudo-reference electrode separated from the bulk solution by a Vycor tip.

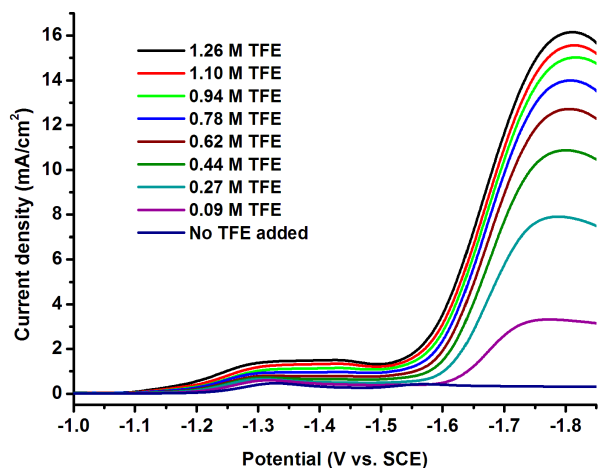


**Figure S4.** Linear scan voltammograms showing the electrocatalytic reduction of  $\text{CO}_2$  to CO by 1 mM  $\text{Mn}(\text{bpy-}t\text{Bu})(\text{CO})_3\text{Br}$  (1) in acetonitrile with addition of trifluoroethanol (TFE). The solution is under an atmosphere of, and saturated with (*ca.* 0.28 M), carbon dioxide. Electrochemical conditions were 0.1 M TBAH as supporting electrolyte, 1 mm diameter glassy carbon working electrode, Pt wire counter electrode, and Ag wire pseudo-reference electrode separated from the bulk solution by a Vycor tip.

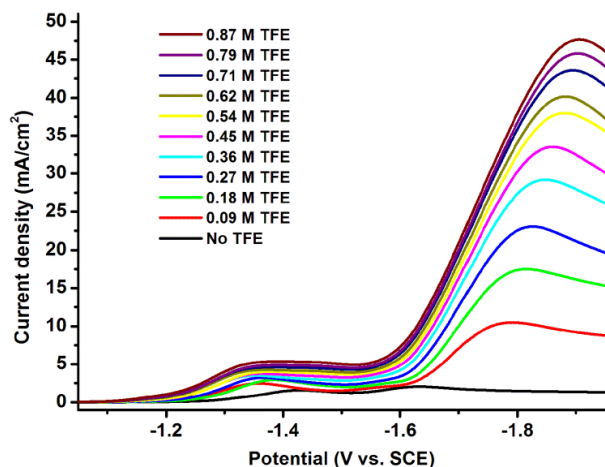


**Figure S5.** Linear scan voltammograms showing the electrocatalytic reduction of  $\text{CO}_2$  to CO by 5 mM  $\text{Mn}(\text{bpy-}t\text{Bu})(\text{CO})_3\text{Br}$  (1) in acetonitrile with addition of trifluoroethanol (TFE). Solution is under an atmosphere of, and saturated with (*ca.* 0.28 M), carbon dioxide. Electrochemical conditions were 0.1 M TBAH as supporting electrolyte, 1 mm diameter glassy carbon working electrode, Pt wire counter electrode, and Ag wire pseudo-reference electrode separated from the bulk solution by a Vycor tip.

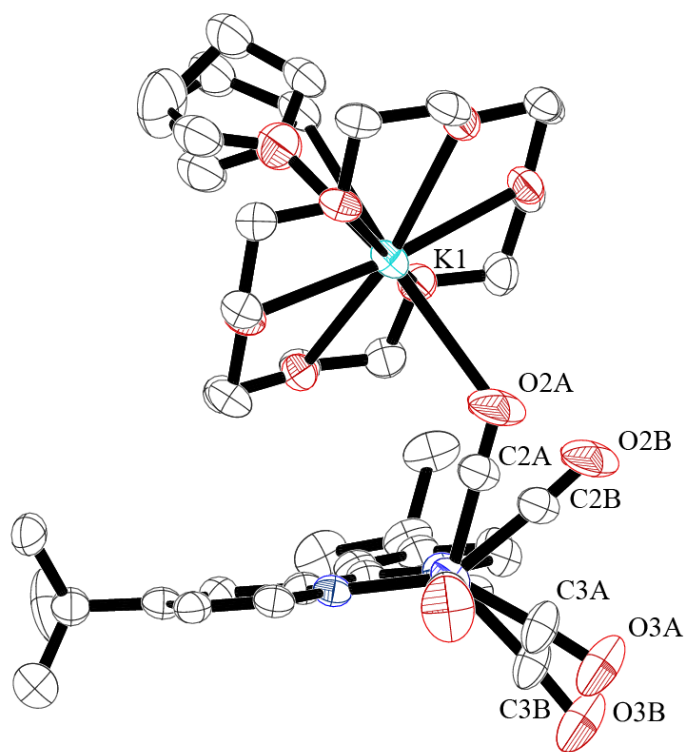


**Figure S6.** Molecular structure of the disordered pair of anions in the crystal structure of  $[\text{Mn}(\text{bpy-}i\text{tBu})(\text{CO})_3][\text{K}(\text{18-crown-6})(\text{THF})]$  (**2**), with hydrogen atoms removed for clarity. Both independent molecules in the unit cell contained disordered THF molecules coordinated to the 18-crown-6 ether encapsulated potassium. This manganese anion contained positional disorder of the carbonyls around the metal center, with the major occupancy modeled at 69%.

**Table S1. Crystallographic data for Mn(bpy-*t*Bu)(CO)<sub>3</sub>Br (1) and [Mn(bpy-*t*Bu)(CO)<sub>3</sub>][K(18-crown-6)(THF)] (2)**

	Mn(bpy- <i>t</i> Bu)(CO) <sub>3</sub> Br (1)	[Mn(bpy- <i>t</i> Bu)(CO) <sub>3</sub> ][K(18-crown-6)(THF)] (2)
Identification code	eb_111026mo_0m	eb_111019_0m
Empirical formula	C21 H24 Br Mn N2 O3	C74 H112 K2 Mn2 N4 O20
Formula weight	487.27	1565.76
Temperature	100(2) K	100(2) K
Wavelength	0.71073 Å	1.54178 Å
Crystal system	Monoclinic	Monoclinic
Space group	P2(1)/n	P2(1)/n
Unit cell dimensions	a = 13.5528(5) Å    α = 90° b = 17.1546(6) Å    β = 96.8790(10)° c = 19.1899(6) Å    γ = 90°	a = 18.2559(4) Å    α = 90° b = 18.4759(4) Å    β = 98.5560(10)° c = 24.2973(5) Å    γ = 90°
Volume	4429.4(3) Å <sup>3</sup>	8104.1(3) Å <sup>3</sup>
Z	8	4
Density (calculated)	1.461 Mg/m <sup>3</sup>	1.283 Mg/m <sup>3</sup>
Absorption coefficient	2.423 mm <sup>-1</sup>	4.023 mm <sup>-1</sup>
F(000)	1984	3328
Crystal size	0.10 x 0.05 x 0.05 mm <sup>3</sup>	0.10 x 0.10 x 0.01 mm <sup>3</sup>
Theta range for data collection	2.11 to 31.78°	2.83 to 50.00°
Index ranges	-19 ≤ h ≤ 19, -25 ≤ k ≤ 23, -22 ≤ l ≤ 28	-13 ≤ h ≤ 18, -18 ≤ k ≤ 18, -24 ≤ l ≤ 24
Reflections collected	45311	28572
Independent reflections	13529 [R(int) = 0.0384]	8004 [R(int) = 0.0488]
Completeness to theta = 25.00°	99.9%	96.1%
Absorption correction	Semi-empirical from equivalents	Semi-empirical from equivalents
Max. and min. transmission	0.8885 and 0.7937	0.9609 and 0.6891
Refinement method	Full-matrix least-squares on F <sup>2</sup>	Full-matrix least-squares on F <sup>2</sup>
Data / restraints / parameters	13529 / 0 / 517	8004 / 0 / 957
Goodness-of-fit on F <sup>2</sup>	1.079	1.026
Final R indices [I > 2σ(I)]	R1 = 0.0407, wR2 = 0.1031	R1 = 0.0733, wR2 = 0.1941
R indices (all data)	R1 = 0.0617, wR2 = 0.1103	R1 = 0.1060, wR2 = 0.2255
Largest diff. peak and hole	0.866 and -0.716 e.Å <sup>-3</sup>	1.401 and -0.301 e.Å <sup>-3</sup>

### Costentin and Savéant TOF calculations<sup>1</sup>

$$\frac{i}{FA} = \frac{\sqrt{k_{cat}D}[C]_p^0}{1 + \exp\left[\frac{F}{RT}(E - E_{CO_2/CO, s, AH}^0)\right]} \quad (1)$$

$$k_{cat} = \frac{i^2 \left(1 + \exp\left[\frac{F}{RT}(E - E_{CO_2/CO, s, AH}^0)\right]\right)^2}{F^2 A^2 D ([C]_p^0)^2} \quad (2)$$

$$\begin{aligned} \text{TOF} &= \frac{k_{cat}}{1 + \exp\left[\frac{F}{RT}(E - E_{CO_2/CO, s, AH}^0)\right]} \\ &\approx k_{cat} \text{ (when } E - E_{cat}^0 < -0.1) \end{aligned} \quad (3)$$

In these equations,  $i$  is Coulombs per second transferred during bulk electrolysis,  $F$  is Faraday's constant,  $A$  is the surface area of the electrode,  $k_{cat}$  is the rate constant of the catalytic reaction,  $D$  is the diffusion coefficient,  $[C]_p^0$  is the concentration of the catalyst without substrate,  $R$  is the universal gas constant,  $T$  is temperature,  $E$  is the applied potential during bulk electrolysis,  $E_{CO_2/CO, s, AH}^0$  is the standard potential for the conversion of  $CO_2$  into  $CO$  in a solvent,  $s$ , and in the presence of an acid,  $AH$ , and TOF is the turnover frequency.

For  $Mn(bpy-tBu)(CO)_3Br$  (1), the values used were:

$$[C]_p^0 = 5.0 \times 10^{-6} \text{ mol cm}^{-3}$$

$$D = 1.1 \times 10^{-5} \text{ cm}^2 \text{ s}^{-1}$$

$$A = 0.0707 \text{ cm}^2$$

$$i = 1.856 \times 10^{-3} \text{ C s}^{-1}$$

$$F = 96845 \text{ C mol}^{-1}$$

$$F/RT = 38.92 \text{ V}^{-1}$$

$$E = -2.2 \text{ V vs. SCE}$$

For these calculations, it was assumed that  $E_{CO_2/CO, s, AH}^0 = -3.1 \text{ V vs. SCE}$ , which is an appropriate value for  $CO_2$  reduction in MeCN solvent.<sup>1</sup> This value is not significant given that the applied potential during bulk electrolysis for Mn catalyst 1 is much less than  $-3.1 \text{ V vs. SCE}$ , and thus, the term  $\exp[(F/RT)(E - E_{CO_2/CO, s, AH}^0)] \approx 0$ . Therefore, the numerator in eqn (2) can be simplified to  $i^2$ . This leads to an equation very similar to the equations described in the main manuscript, and a calculated TOF of  $267 \text{ s}^{-1}$  for catalyst 1 in the presence of  $1.26 \text{ M TFE}$ .

(1) Costentin, C.; Drouet, S.; Robert, M.; Savéant, J.-M. *Science* **2012**, 338, 90.

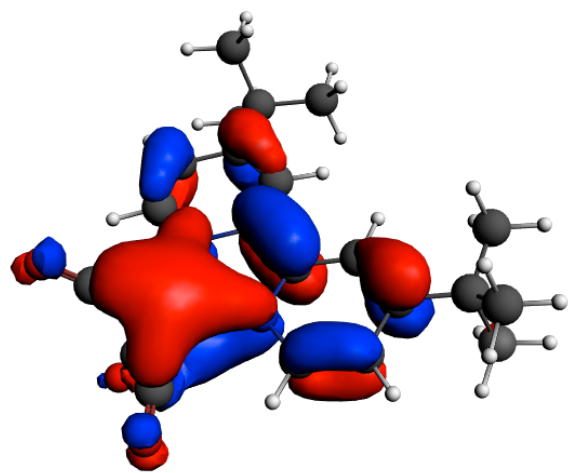


**Figure S7.** The representation of the DFT-calculated HOMO of  $[\text{Mn}(\text{bpy-}t\text{Bu})(\text{CO})_3]^{-1}$  calculated using ADF 2007.01.



**Table S3. Comparison of selected experimental and DFT-calculated bond lengths (Å) and angles (°) for [Mn(bpy-*t*Bu)(CO)<sub>3</sub>]<sup>−</sup>**

Bond(s)	Exp. <sup>a</sup>	DFT/BP86
Mn2–N3	1.982	1.997
Mn2–N4	1.992	2.013
Mn2–C22	1.774	1.792
Mn2–C23	1.785	1.795
Mn2–C24	1.767	1.787
O4–C22	1.171	1.177
O5–C23	1.186	1.178
O6–C24	1.191	1.179
N3–C25	1.376	1.372
N3–C29	1.396	1.402
N4–C30	1.387	1.392
N4–C34	1.361	1.363
C25–C26	1.351	1.370
C26–C27	1.441	1.436
C27–C28	1.441	1.379
C28–C29	1.401	1.416
C29–C30	1.411	1.413
C30–C31	1.431	1.418
C31–C32	1.361	1.379
C32–C33	1.431	1.434
C33–C34	1.351	1.375
C22–Mn2–C23	97.24	89.58
C22–Mn2–C24	91.34	95.43
C23–Mn2–C24	88.94	91.58
N3–Mn2–N4	78.82	78.41
N3–Mn2–C22	122.93	140.59
N3–Mn2–C23	122.93	123.76
N3–Mn2–C24	93.03	92.99
N4–Mn2–C22	95.83	96.93
N4–Mn2–C23	94.63	94.24
N4–Mn2–C24	171.73	170.30

<sup>a</sup> Experimental structure of [Mn(bpy-*t*Bu)(CO)<sub>3</sub>][K(18-crown-6)(THF)]

**Table S4. Output xyz coordinates from the DFT Geometry Optimization calculation of [Mn(bpy-*t*Bu)(CO)<sub>3</sub>]<sup>−</sup>**

Atom	X	Y	Z
Mn	14.890702	3.097274	0.073220
O	13.854762	1.245955	-1.996049
O	12.207178	4.066724	0.897824
O	14.747095	0.959568	2.134851
N	16.830903	3.428762	0.408004
N	15.248656	4.662889	-1.140113
C	14.275605	1.986711	-1.183700
C	13.277467	3.689192	0.580677
C	14.798064	1.813013	1.323526
C	17.664800	2.737239	1.250279
H	17.205782	1.907132	1.780148
C	18.987119	3.031370	1.454654
H	19.547218	2.410431	2.153909
C	19.606558	4.135736	0.777632
C	18.793488	4.822239	-0.099578
H	19.182346	5.669547	-0.661128
C	17.434742	4.477007	-0.300990
C	16.556229	5.138690	-1.187684
C	16.922160	6.171541	-2.087587
H	17.966519	6.475558	-2.106791
C	16.008511	6.767407	-2.931349
C	14.661106	6.286449	-2.837356
H	13.863907	6.704947	-3.452087
C	14.350293	5.268887	-1.966906
H	13.334374	4.884705	-1.901505
C	21.087373	4.459790	0.997837
C	21.420706	4.477549	2.506738
H	20.846245	5.258731	3.025648
H	22.494628	4.675743	2.657993
H	21.187167	3.517122	2.985199
C	21.949663	3.373536	0.310135
H	21.675305	2.370716	0.666964
H	23.021625	3.534496	0.514848
H	21.794628	3.394819	-0.779086
C	21.474908	5.830151	0.414892
H	21.326313	5.866684	-0.672651
H	22.538713	6.033181	0.613036
H	20.881583	6.636891	0.868102
C	16.373833	7.870425	-3.929203
C	17.878823	8.190729	-3.914449
H	18.214779	8.514567	-2.919652
H	18.093833	9.003469	-4.625293
H	18.475274	7.315749	-4.211652
C	15.996635	7.428706	-5.362037
H	16.533032	6.509435	-5.635607
H	16.259873	8.212707	-6.090831
H	14.920837	7.228061	-5.451386
C	15.597004	9.162081	-3.581497
H	14.511983	8.989670	-3.592782
H	15.824444	9.960057	-4.306318
H	15.868241	9.518040	-2.577465